

GraphGen: A Scalable Approach to Domain-agnostic Labeled Graph Generation

Nikhil Goyal*

Indian Institute of Technology, Delhi
nikhil10sep@gmail.com

Harsh Vardhan Jain*

Indian Institute of Technology, Delhi
harshvardhanjain7@gmail.com

Sayan Ranu

Indian Institute of Technology, Delhi
sayanranu@cs.iitd.ac.in

Abstract

Graph generative models have been extensively studied in the data mining literature. While traditional techniques are based on generating structures that adhere to a pre-decided distribution, recent techniques have shifted towards *learning* this distribution directly from the data. While learning-based approaches have imparted significant improvement in quality, some limitations remain to be addressed. First, learning graph distributions introduces additional computational overhead, which limits their scalability to large graph databases. Second, many techniques only learn the structure and do not address the need to also learn node and edge labels, which encode important semantic information and influence the structure itself. Third, existing techniques often incorporate domain-specific rules and lack generalizability. Fourth, the experimentation of existing techniques is not comprehensive enough due to either using weak evaluation metrics or focusing primarily on synthetic or small datasets. In this work, we develop a *domain-agnostic* technique called GRAPHGEN to overcome all of these limitations. GRAPHGEN converts graphs to sequences using *minimum DFS codes*. Minimum DFS codes are *canonical labels* and capture the graph structure precisely along with the label information. The complex joint distributions between structure and semantic labels are learned through a novel LSTM architecture. Extensive experiments on million-sized, real graph datasets show GRAPHGEN to be 4 times faster on average than state-of-the-art techniques while being significantly better in quality across a comprehensive set of 11 different metrics. Our code is released at: <https://github.com/idea-iitd/graphgen>.

ACM Reference Format:

Nikhil Goyal, Harsh Vardhan Jain, and Sayan Ranu. 2020. GraphGen: A Scalable Approach to Domain-agnostic Labeled Graph Generation. In *Proceedings of The Web Conference 2020 (WWW '20)*, April 20–24, 2020, Taipei, Taiwan. ACM, New York, NY, USA, 11 pages. <https://doi.org/10.1145/3366423.3380201>

1 Introduction and Related Work

Modeling and generating real-world graphs have applications in several domains, such as understanding interaction dynamics in social networks[12, 35, 36], graph classification[3, 25, 27], and anomaly detection[26]. Owing to their wide applications, development of generative models for graphs has a rich history, and many methods have been proposed. However, a majority of the techniques, make

*Both authors contributed equally to this research.

This paper is published under the Creative Commons Attribution 4.0 International (CC-BY 4.0) license. Authors reserve their rights to disseminate the work on their personal and corporate Web sites with the appropriate attribution.

WWW '20, April 20–24, 2020, Taipei, Taiwan

© 2020 IW3C2 (International World Wide Web Conference Committee), published under Creative Commons CC-BY 4.0 License.

ACM ISBN 978-1-4503-7023-3/20/04.

<https://doi.org/10.1145/3366423.3380201>

Table 1: Limitations of existing graph generative models. n and m denote the number of nodes and edges respectively. Any other variable is a hyper-parameter of the respective model. We consider a model scalable if its complexity is linear in n and m .

Technique	Domain-agnostic	Node Labels	Edge Labels	Scalable	Complexity
MolGAN[7]	✗	✓	✓	✗	$O(n^2)$
NeVAE[31]	✗	✓	✓	✓	$O(Sm)$
GCPN[39]	✗	✓	✓	✗	$O(m^2)$
LGGAN[8]	✓	✓	✗	✗	$O(n^2)$
Graphite[12]	✓	✓	✗	✗	$O(n^2)$
DeepGMG[19]	✓	✓	✓	✗	$O(n^2m)$
GraphRNN[40]	✓	✗	✗	✓	$O(nM)$
GraphVAE[34]	✓	✓	✓	✗	$O(n^4)$
GRAN[21]	✓	✗	✗	✗	$O(n(m+n))$
GRAPHGEN	✓	✓	✓	✓	$O(m)$

assumptions about certain properties of the graph database, and generate graphs that adhere to those assumed properties[1, 2, 18, 28, 41]. A key area that lacks development is the ability to directly *learn* patterns, both local as well as global, from a given set of observed graphs and use this knowledge to generate graphs instead of making prior assumptions. In this work, we bridge this gap by developing a domain-agnostic graph generative model for labeled graphs without making any prior assumption about the dataset. Such an approach reduces the usability barrier for non-technical users and applies to domains where distribution assumptions made by traditional techniques do not fit well, e.g. chemical compounds, protein interaction networks *etc.*

Modeling graph structures is a challenging task due to the inherent complexity of encoding both local and global dependencies in link formation among nodes. We briefly summarize how existing techniques tackle this challenge and their limitations.

Traditional graph generative models: Several models exist[1, 2, 18, 28, 29, 37] that are engineered towards modeling a pre-selected family of graphs, such as random graphs[28], small-world networks[37], and scale-free graphs[2]. The apriori assumption introduces several limitations. First, due to pre-selecting the family of graphs, *i.e.* distributions modeling some structural properties, they cannot adapt to datasets that either do not fit well or evolve to a different structural distribution. Second, these models only incorporate structural properties and do not look into the patterns encoded by labels. Third, these models assume the graph to be homogeneous. In reality, it is possible that different local communities (subgraphs) within a graph adhere to different structural distributions.

Learning-based graph generative models: To address the above outlined limitations, recent techniques have shifted towards a learning-based approach[8, 16, 19, 21, 34, 40]. While impressive progress has been made through this approach, there is scope to further improve the performance of graph generative models. We outline the key areas we target in this work.

- **Domain-agnostic modeling:** Several models have been proposed recently that target graphs from a specific domain and employ domain-specific constraints[7, 15, 20, 22, 24, 31, 39] in the generative task. While these techniques produce excellent results on the target domain, they do not generalize well to graphs from other domains.
- **Labeled graph generation:** Real-world graphs, such as protein interaction networks, chemical compounds, and knowledge graphs, encode semantic information through node and edge labels. To be useful in these domains, we need a generative model that jointly captures the relationship between structure and labels (both node and edge labels).
- **Data Scalability:** It is not uncommon to find datasets containing millions of graphs[14]. Consequently, it is important for any generative model to scale to large training datasets so that all of the information can be exploited for realistic graph generation. Many of the existing techniques do not scale to large graph databases[8, 19, 21, 34, 40]. Often this non-scalability stems from dealing with exponential representations of the same graph, complex neural architecture, and large parameter space. For example, LGGAN[8] models graph through its adjacency matrix and therefore has $O(n^2)$ complexity, where n is the number of nodes in the graph. GraphRNN[40] is the most scalable among existing techniques due to employing a smaller recurrent neural network (RNN) of $O(nM)$ complexity, where M is a hyper-parameter. In GraphRNN, the sequence representations are constructed by performing a large number of breadth-first-search (BFS) enumerations for each graph. Consequently, even if the size of the graph dataset is small, the number of unique sequences fed to the neural network is much larger, which in turn affects scalability.

Table 1 summarizes the limitations of learning-based approaches. GRAPHGEN addresses all of the above outlined limitations and is the first technique that is domain-agnostic, assumption-free, models both labeled and unlabeled graphs, and data scalable. Specifically, we make the following contributions.

- We propose the problem of learning a graph generative model that is assumption-free, domain-agnostic, and captures the complex interplay between semantic labels and graph structure (§ 2).
- To solve the proposed problem, we develop an algorithm called GRAPHGEN that employs the unique combination of *graph canonization* with deep learning. Fig. 1 outlines the pipeline. Given a database of training graphs, we first construct the canonical label of each graph[17, 38]. The canonical label of a graph is a string representation such that two graphs are *isomorphic* if and only if they have the same canonical label. We use *DFS codes* for canonization. Through canonization, the graph generative modeling task converts to a sequence modeling task, for which we use Long Short-term Memory (LSTM)[13] (§ 3).
- We perform an extensive empirical evaluation on real million-sized graph databases spanning three different domains. Our empirical evaluation establishes that we are significantly better in quality than the state-of-the-art techniques across an array of metrics, more robust, and 4 times faster on average (§ 4).

2 Problem Formulation

As a notational convention, a graph is represented by the tuple $G = (V, E)$ consisting of node set $V = \{v_1, \dots, v_n\}$ and edge set

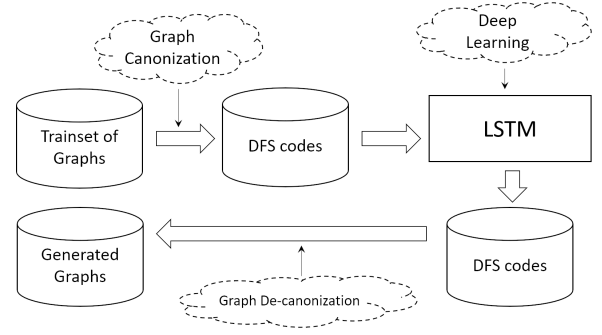


Figure 1: Flowchart of GRAPHGEN.

$E = \{(v_i, v_j) | v_i, v_j \in V\}$. Graphs may be annotated with node and edge labels. Let $\mathcal{L}_n : V \rightarrow \mathbb{V}$ and $\mathcal{L}_e : E \rightarrow \mathbb{E}$ be the node and edge label mappings respectively where \mathbb{V} and \mathbb{E} are the set of all node and edge labels respectively. We use the notation $L(v)$ and $L(e)$ to denote the labels of node v and edge e respectively. We assume that the graph is connected and there are no self-loops.

The goal of a graph generative model is to learn a distribution $p_{model}(\mathbb{G})$ over graphs, from a given set of observed graphs $\mathbb{G} = \{G_1, G_2, \dots, G_m\}$ that is drawn from an underlying hidden distribution $p(\mathbb{G})$. Each G_i could have a different number of nodes and edges, and could possibly have a different set of node labels and edge labels. The graph generative model is effective if the learned distribution is similar to the hidden distribution, *i.e.*, $p_{model}(\mathbb{G}) \approx p(\mathbb{G})$. More simply, the learned generative model should be capable of generating *similar* graphs of varied sizes from the same distribution as $p(\mathbb{G})$ without any prior assumption about structure or labeling.

2.1 Challenges

- **Large and variable output space:** The structure of a graph containing n nodes can be characterized using an $n \times n$ adjacency matrix, which means a large output space of $O(n^2)$ values. With node and edge labels, this problem becomes even more complex as the adjacency matrix is no longer binary. Furthermore, the mapping from a graph to its adjacency matrix is not one-to-one. A graph with n nodes can be equivalently represented using $n!$ adjacency matrices corresponding to each possible node ordering. Finally, n itself varies from graph to graph.
- **Joint distribution space:** While we want to learn the hidden graph distribution $p(G)$, defining $p(G)$ itself is a challenge since graph structures are complex and composed of various properties such as node degree, clustering coefficients, node and edge labels, number of nodes and edges, *etc.* One could learn a distribution over each of these properties, but that is not enough since these distributions are not independent. The key challenge is therefore to learn the complex dependencies between various properties.
- **Local and global dependencies:** The joint distribution space itself may not be homogeneous since the dependence between various graph parameters varies across different regions of a graph. For example, not all regions of a graph are equally dense. We overcome these challenges through GRAPHGEN.

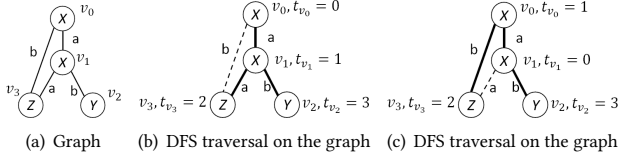


Figure 2: Illustrates the DFS code generation process.

3 GRAPHGEN: Generative model for labeled graphs

Instead of using adjacency matrices to capture graph structures, we perform graph canonization to convert each graph into a unique sequence. This step provides two key advantages. First, the length of the sequence is $|E|$ for graph $G(V, E)$ instead of $|V|^2$. Although in the worst case, $|E| = |V|^2$, in real graphs, this is rarely seen. Second, there is a one-to-one mapping between a graph and its canonical label instead of $|V|!$ mappings. Consequently, the size of the output space is significantly reduced, which results in faster and better modeling.

3.1 DFS Codes: Graphs to Sequences

First, we formally define the concept of *graph canonization*.

DEFINITION 1 (GRAPH ISOMORPHISM). Graph $G_1 = (V_1, E_1)$ is isomorphic to $G_2 = (V_2, E_2)$ if there exists a bijection ϕ such that for every vertex $v \in V_1$, $\phi(v) \in V_2$ and for every edge $e = (u, v) \in E_1$, $\phi(e) = (\phi(u), \phi(v)) \in E_2$. If the graphs are labeled, we also need to ensure that the labels of mapped nodes and edges are the same, i.e., $\mathcal{L}(v) = \mathcal{L}(\phi(v))$ and $\mathcal{L}(e) = \mathcal{L}(\phi(e))$.

DEFINITION 2 (CANONICAL LABEL). The canonical label of a graph is a string representation such that two graphs have the same label if and only if they are isomorphic to each other.

We use *DFS codes*[38] to construct graph canonical labels. DFS code encodes a graph into a unique edge sequence by performing a depth first search (DFS). The DFS traversal may start from any node in the graph. To illustrate, consider Fig. 2(a). A DFS traversal starting at v_0 on this graph is shown in Fig. 2(b) where the bold edges show the edges that are part of the DFS traversal. During the DFS traversal, we assign each node a *timestamp* based on when it is discovered; the starting node has the timestamp 0. Fig. 2(b) shows the timestamps if the order of DFS traversal is (v_0, v_1) , (v_1, v_3) , (v_1, v_2) . We use the notation t_u to denote the timestamp of node u . Any edge (u, v) that is part of the DFS traversal is guaranteed to have $t_u < t_v$, and we call such an edge a *forward edge*. On the other hand, the edges that are not part of the DFS traversal, such as (v_3, v_0) in Fig. 2(b), are called *backward edges*. In Fig. 2(b), the bold edges represent the forward edges, and the dashed edge represents the backward edge. Based on the timestamps assigned, an edge (u, v) is described using a 5-tuple $(t_u, t_v, L_u, L_{(u,v)}, L_v)$, where L_u and $L_{(u,v)}$ denote the node and edge labels of u and (u, v) respectively.

Given a DFS traversal, our goal is to impose a *total ordering* on all edges of the graph. Forward edges already have an ordering between them based on when they are traversed in DFS. To incorporate backward edges, we enforce the following rule:

- Any backward edge (u, u') must be ordered before all forward edges of the form (u, v) .

- Any backward edge (u, u') must be ordered after the forward edge of the form (w, u) , i.e., the first forward edge pointing to u .
- Among the backward edges from the same node u of the form (u, u') and (u, u'') , (u, u'') has a higher order if $t_{u''} < t_{u'}$.

With the above rules, corresponding to any DFS traversal of a graph, we can impose a total ordering on all edges of a graph and can thus convert it to a sequence of edges that are described using their 5-tuple representations. We call this sequence representation a *DFS code*.

Example 3.1. Revisiting Fig. 2(b), the DFS code is $\langle (0, 1, X, a, X) (1, 2, X, a, Z) (2, 0, Z, b, X) (1, 3, X, b, Y) \rangle$. A second possible DFS traversal is shown in Fig. 2(c), for which the edge sequence is $\langle (0, 1, X, a, X) (1, 2, X, b, Z) (2, 0, Z, a, X) (0, 3, X, b, Y) \rangle$.

Since each graph may have multiple DFS traversals, we choose the *lexicographically smallest* DFS code based upon the lexicographical ordering proposed in[38]. Hereon, the lexicographically smallest DFS code is referred to as the *minimum DFS code*. We use the notation $\mathcal{F}(G) = S = [s_1, \dots, s_m]$ to denote the *minimum DFS code* of graph G , where $m = |E|$.

THEOREM 1. $\mathcal{F}(G)$ is a canonical label for any graph G . [38]

Example 3.2. The DFS code for Fig. 2(b) is smaller than Fig. 2(c) since the second edge tuple $(1, 2, X, a, Z)$ of Fig. 2(b) is smaller than $(1, 2, X, b, Z)$ of Fig. 2(c) as $a < b$. Since the first edge tuple in both sequences are identical the tie is broken through the second tuple.

3.1.1 Computation Cost and Properties Constructing the minimum DFS code of a graph is equivalent to solving the graph isomorphism problem. Both operations have a worst-case computation cost of $O(|V|!)$ since we may need to evaluate all possible permutations of the nodes to identify the lexicographically smallest one. Therefore an important question arises: *How can we claim scalability with a factorial computation complexity?* To answer this question, we make the following observations.

- **Labeled graphs are ubiquitous:** Most real graphs are labeled. Labels allow us to drastically prune the search space and identify the minimum DFS code quickly. For example, in Fig. 2(a), the only possible starting nodes are v_0 or v_1 as they contain the lexicographically smallest node label “X”. Among them, their 2-hop neighborhoods are enough to derive that v_0 must be the starting node of the minimum DFS code as $(1, 2, X, a, Z)$ is the lexicographically smallest possible tuple after $(0, 1, X, a, X)$ in the graph in Fig. 2(a). We empirically substantiate this claim in § 4.3.2.
- **Invariants:** What happens if the graph is unlabeled or has less diversity in labels? In such cases, *vertex and edge invariants* can be used as node and edge labels. Invariants are properties of nodes and edges that depend only on the structure and not on graph representations such as adjacency matrix or edge sequence. Examples include node degree, betweenness centrality, clustering coefficient, etc. We empirically study this aspect further in § 4.4.
- **Precise training:** Existing techniques rely on the neural network to learn the multiple representations that correspond to the same graph. Many-to-one mappings introduce impreciseness and bloat the modeling task with redundant information. In GRAPHGEN, we feed precise one-to-one graph representations, which allows us to use a more lightweight neural architecture. Dealing

with multiple graph representations are handled algorithmically, which leads to significant improvement in quality and scalability.

3.2 Modeling Sequences

3.2.1 Model Overview Owing to the conversion of graphs to minimum DFS codes, and given that DFS codes are canonical labels, modeling a database of graphs $\mathbb{G} = \{G_1, \dots, G_n\}$ is equivalent to modeling their sequence representations $\mathbb{S} = \{\mathcal{F}(G_1), \dots, \mathcal{F}(G_n)\} = \{S_1, \dots, S_n\}$, i.e., $p_{model}(\mathbb{G}) \equiv p_{model}(\mathbb{S})$. To model the sequential nature of the DFS codes, we use an *auto-regressive* model to learn $p_{model}(\mathbb{S})$. At inference time, we sample DFS codes from this distribution instead of directly sampling graphs. Since the mapping of a graph to its minimum DFS code is a *bijection*, i.e., $G = \mathcal{F}^{-1}(\mathcal{F}(G))$, the graph structure along with all node and edge labels can be fully constructed from the sampled DFS code.

Fig.3 provides an overview of GRAPHGEN model. For graph $G(V, E)$ with $\mathcal{F}(G) = S = [s_1, \dots, s_m]$, the proposed auto-regressive model generates s_i sequentially from $i = 1$ to $i = m = |E|$. This means that our model produces a single edge at a time, and since it belongs to a DFS sequence, it can only be between two previously generated nodes (backward edge) or one of the already generated nodes and an unseen node (forward edge), in which case a new node is also formed. Consequently, only the first generated edge produces two new nodes, and all subsequent edges produce at most one new node.

3.2.2 Model Details We now describe the proposed algorithm to characterize $p(S)$ in detail. Since S is sequential in nature, we decompose the probability of sampling S from $p(\mathbb{S})$ as a product of *conditional distribution* over its elements as follows:

$$p(S) = \prod_{i=1}^{m+1} p(s_i | s_1, \dots, s_{i-1}) = \prod_{i=1}^{m+1} p(s_i | s_{<i}) \quad (1)$$

where m is the number of edges and s_{m+1} is *end-of-sequence* token EOS to allow variable length sequences. We denote $p(s_i | s_1, \dots, s_{i-1})$ as $p(s_i | s_{<i})$ in further discussions.

Recall, each element s_i is an edge tuple of the form $(t_u, t_v, L_u, L_e, L_v)$, where $e = (u, v)$. We make the simplifying assumption that timestamps t_u, t_v , node labels L_u, L_v and edge label L_e at each generation step of s_i are independent of each other. This makes the model tractable and easier to train. Note that this assumption is not dependent on data and hence is not forming prior bias of any sort on data. Mathematically, Eq. 1 reduces to the follows.

$$\begin{aligned} p(s_i | s_{<i}) &= p((t_u, t_v, L_u, L_e, L_v) | s_{<i}) \\ &= p(t_u | s_{<i}) \times p(t_v | s_{<i}) \times p(L_u | s_{<i}) \\ &\quad \times p(L_e | s_{<i}) \times p(L_v | s_{<i}) \end{aligned} \quad (2)$$

Eq. 2 is extremely complex as it has to capture complete information about an upcoming edge, i.e., the nodes to which the edge is connected, their labels, and the label of the edge itself. To capture this highly complex nature of $p(s_i | s_{<i})$ we propose to use expressive neural networks. *Recurrent neural networks (RNNs)* are capable of learning features and long term dependencies from sequential and time-series data[30]. Specifically, LSTMs[13] have been one of the most popular and efficient methods for reducing the effects of vanishing and exploding gradients in training RNNs. In recent

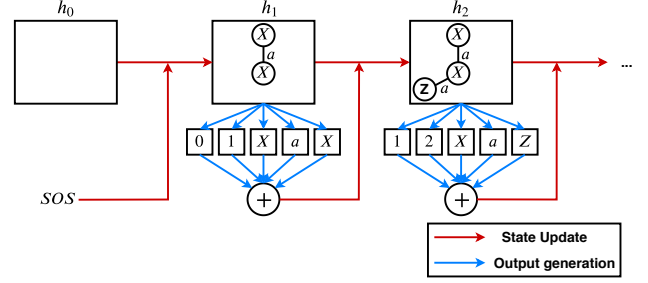


Figure 3: Architecture of GRAPHGEN. Red arrows indicate data flow in the RNN whose hidden state h_i captures the state of the graph generated so far. Blue arrows show the information flow to generate the new edge tuple s_i .

times, LSTMs and *stacked* LSTMs have delivered promising results in cursive handwriting[9], sentence modeling[5] and, speech recognition[10].

In this paper, we design a custom LSTM that consists of a *state transition function* f_{trans} (Eq. 3), an embedding function f_{emb} (Eq. 3), and five separate *output functions* (Eqs. 4-8) for each of the five components of the 5-tuple $s_i = (t_u, t_v, L_u, L_e, L_v)$. (\sim_M in the following equations represents sampling from multinomial distribution)

$$h_i = f_{trans}(h_{i-1}, f_{emb}(s_{i-1})) \quad (3)$$

$$t_u \sim_M \theta_{t_u} = f_{t_u}(h_i) \quad (4)$$

$$t_v \sim_M \theta_{t_v} = f_{t_v}(h_i) \quad (5)$$

$$L_u \sim_M \theta_{L_u} = f_{L_u}(h_i) \quad (6)$$

$$L_e \sim_M \theta_{L_e} = f_{L_e}(h_i) \quad (7)$$

$$L_v \sim_M \theta_{L_v} = f_{L_v}(h_i) \quad (8)$$

$$s_i = \text{concat}(t_u, t_v, L_u, L_e, L_v) \quad (9)$$

Here, $s_i \in \{0, 1\}^k$ is the concatenated component wise *one-hot encoding* of the real edge, and $h_i \in \mathbb{R}^d$ is an LSTM hidden state vector that encodes the state of the graph generated so far. An embedding function f_{emb} is used to compress the sparse information possessed by the large edge representation (s_i) to a small vector of real numbers (Eq. 3). Given the graph state, h_i , the output of the functions $f_{t_u}(h_i), f_{t_v}(h_i), f_{L_u}(h_i), f_{L_e}(h_i), f_{L_v}(h_i)$ i.e. $\theta_{t_u}, \theta_{t_v}, \theta_{L_u}, \theta_{L_e}, \theta_{L_v}$ respectively represent the multinomial distribution over possibilities of five components of the newly formed edge tuple. Finally, components of the newly formed edge tuple are sampled from the multinomial distributions parameterized by respective θ s and concatenated to form the new edge (s_i) (Eq. 9).

With the above design, the key components that dictate the modeling quality are the multinomial probability distribution parameters $\theta_{t_u}, \theta_{t_v}, \theta_{L_u}, \theta_{L_e}, \theta_{L_v}$ over each edge tuple t_u, t_v, L_u, L_e, L_v . Our goal is, therefore, to ensure that the learned distributions are as close as possible to the real distributions in the training data. Using the broad mathematical architecture explained above, we will now explain the Graph Generation process followed by the sequence modeling / training process.

3.2.3 Graph Generation Given the learned state transition function f_{trans} , embedding function f_{emb} and output functions f_{t_u} , f_{t_v} , f_{L_u} , f_{L_e} , f_{L_v} , Alg. 1 provides the pseudocode for the graph generation process. In Alg. 1, S stores the generated sequence and is initialized along with other variables (line 1-3). $\widehat{s}_i \in \{0, 1\}^k$, which represents i^{th} edge tuple formed for sequence S , is component-wise sampled from the multinomial distributions learned by output functions (loop at line 8) and finally appended to the sequence S (line 13). This process of forming a new edge and appending it to sequence S is repeated until any of the five components is sampled as an EOS. Note, since each of the five components of \widehat{s}_i i.e., $c_i, c \in \{t_u, t_v, L_u, L_e, L_v\}$ are one-hot encodings and can be of different size, their EOS could be of different sizes, in which case they will be compared with their respective EOS to indicate the stopping condition.

3.2.4 Graph Modeling We now discuss how the required inference functions (Eqs. 3-9) are learned from a set of training graphs.

Given an input graph dataset \mathbb{G} , Alg. 2 first converts the graph dataset \mathbb{G} to a sequence dataset \mathbb{S} of minimum DFS codes (line 1). We initialize the unlearned neural functions by suitable weights (line 2). Further details about these functions are given in Sec. 3.2.5. For each edge s_i in each sequence $S \in \mathbb{S}$, a concatenated component-wise one-hot encoding of the real edge s_i is fed to the embedding function f_{emb} , which compresses it and its compressed form along with previous graph state is passed to the transition function f_{trans} . f_{trans} generates the new graph state h_i (line 8). This new state h_i is passed to all the five output functions that provide us the corresponding probability distributions over the components of the new edge tuple (line 11). We concatenate these probability distributions to form $\widehat{s}_i \in \mathbb{R}^k$ (same size as that of s_i), which is representative of a new edge (line 12). Finally, this component-wise concatenated probability distribution \widehat{s}_i is matched (component-wise) against the real tuple from the DFS code being learned. This implies that we use ground truth rather than the model’s own prediction during successive time steps in training. In contrast to this, GRAPHGEN uses its own predictions during graph generation time. The accuracy of the model is optimized using the cumulative *binary cross-entropy* loss function. Here $s[c]$ represents component $c \in \{t_u, t_v, L_u, L_e, L_v\}$, and \log is taken elementwise on a vector.

Algorithm 1: Graph generation algorithm

```

Input :LSTM based state transition function  $f_{trans}$ , embedding function  $f_{emb}$ , five
output functions  $f_{t_u}, f_{t_v}, f_{L_u}, f_{L_e}, f_{L_v}$ , empty graph state  $h_0$ , start token
SOS, and end token EOS
Output:Graph G
1  $S \leftarrow \emptyset$ 
2  $\widehat{s}_0 \leftarrow SOS$ 
3  $i \leftarrow 0$ 
4 repeat
5    $i \leftarrow i + 1$ 
6    $h_i \leftarrow f_{trans}(h_{i-1}, f_{emb}(\widehat{s}_{i-1}))$ 
7    $\widehat{s}_i \leftarrow \emptyset$ 
8   for  $c \in \{t_u, t_v, L_u, L_e, L_v\}$  do
9      $\theta_c \leftarrow f_c(h_i)$ 
10    // sample  $c_i$  from Multinomial distribution parameterized by  $\theta_c$ 
11     $c_i \sim_M \theta_c$ 
12     $\widehat{s}_i \leftarrow \text{concat}(\widehat{s}_i, c_i)$ 
13  end
14   $S \leftarrow S || (\widehat{s}_i)$  // Appending  $\widehat{s}_i$  to sequence S
15 until  $\exists c_i, c_i = EOS$ 
16 return  $\mathcal{F}^{-1}(S)$  //  $\mathcal{F}^{-1}$  is mapping from minimum DFS code to graph

```

Table 2: Variables and their sizes

Variable (One-hot vector)	Dimension
t_u, t_v	$\max_{\forall G(V,E) \in \mathbb{G}} V + 1$
L_u, L_v	$ V + 1$
L_e	$ E + 1$

$$BCE(\widehat{s}_i, s_i) = - \sum_c \left(s_i[c]^T \log \widehat{s}_i[c] + (1 - s_i[c])^T \log(1 - \widehat{s}_i[c]) \right) \quad (10)$$

3.2.5 Parameters State transition function, f_{trans} in our architecture is a stacked LSTM-Cell, each of the five output functions $f_{t_u}, f_{t_v}, f_{L_u}, f_{L_e}, f_{L_v}$ are fully connected, independent *Multi-layer Perceptrons (MLP)* with dropouts and f_{emb} is a simple linear embedding function. The dimension of the one-hot encodings of t_u, t_v, L_u, L_e, L_v are estimated from the training set. Specifically, the largest values for each element are computed in the first pass while computing the minimum DFS codes of the training graphs. Table 2 shows the dimensions of the one-hot encodings for each component of s_i . Note that each variable has one size extra than their intuitive size to incorporate the EOS token. Since we set the dimensions of t_u and t_v to the largest training graph size, in terms of the number of nodes, the largest generated graph cannot exceed the largest training graph. Similarly, setting the dimensions of L_u, L_v , and L_e to the number of unique node and edge labels in the training set means that our model is bound to produce only labels that have been observed at least once. Since the sizes of each component of s_i is fixed, the size of s_i , which is formed by concatenating these components, is also fixed, and therefore, satisfies the pre-requisite condition for LSTMs to work, i.e., each input must be of the same size. We employ weight sharing among all time steps in LSTM to make the model scalable.

3.2.6 Complexity Analysis of Modeling and Inference. Consistent with the complexity analysis of existing models (Recall Table 1), we only analyze the complexity of the forward and backward propagations. The optimization step to learn weights is not included.

Algorithm 2: Graph modeling algorithm

```

Input :Dataset of Graphs  $\mathbb{G} = \{G_1, \dots, G_n\}$ 
Output :Learned functions  $f_{trans}, f_{t_u}, f_{t_v}, f_{L_u}, f_{L_e}, f_{L_v}$ , and embedding function
 $f_{emb}$ 
1  $\mathbb{S} = \{S = \mathcal{F}(G) \mid \forall G \in \mathbb{G}\}$ 
2 Initialize  $f_{t_u}, f_{t_v}, f_{L_u}, f_{L_e}, f_{L_v}, f_{emb}$  // 1 Epoch
3 repeat
4   for  $\forall S = [s_1, \dots, s_m] \in \mathbb{S}$  do
5      $s_0 \leftarrow SOS$ ; Initialize  $h_0$ 
6      $loss \leftarrow 0$ 
7     for  $i$  from 1 to  $m + 1$  do //  $s_{m+1}$  for EOS tokens
8        $h_i \leftarrow f_{trans}(h_{i-1}, f_{emb}(s_{i-1}))$ 
9       //  $\widehat{s}_i$  will contain component-wise probability distribution
10      // vectors of  $\widehat{s}_i$ 
11       $\widehat{s}_i \leftarrow \phi$ 
12      for  $c \in \{t_u, t_v, L_u, L_e, L_v\}$  do
13         $\theta_c \leftarrow f_c(h_i)$ 
14         $\widehat{s}_i \leftarrow \text{concat}(\widehat{s}_i, \theta_c)$ 
15      end
16      // Note:  $s_i$  consists of 5 components (See Eq. 10)
17       $loss \leftarrow loss + BCE(\widehat{s}_i, s_i)$ 
18    end
19  end
20 until stopping criteria // Typically when validation loss is minimized

```

Table 3: Summary of the datasets. X means labels are absent.

#	Name	Domain	No. of graphs	$ V $	$ E $	$ V $	$ E $
1	NCI-H23 (Lung)[23]	Chemical	24k	[6, 50]	[6, 57]	11	3
2	Yeast[23]	Chemical	47k	[5, 50]	[5, 57]	11	3
3	MOLT-4 (Leukemia)[23]	Chemical	33k	[6, 111]	[6, 116]	11	3
4	MCF-7 (Breast)[23]	Chemical	23k	[6, 111]	[6, 116]	11	3
5	ZINC[14]	Chemical	3.2M	[3, 42]	[2, 49]	9	4
6	Enzymes[4]	Protein	575	[2, 125]	[2, 149]	3	X
7	Citeseer[33]	Citation	1	3312	4460	6	X
8	Cora[33]	Citation	1	2708	5278	6	X

The length of the sequence representation for graph $G(V, E)$ is $|E|$. All operations in the LSTM model consume $O(1)$ time per edge tuple and hence the complexity is $O(|E|)$. The generation algorithm consumes $O(1)$ time per edge tuple and for a generated graph with edge set E , the complexity is $O(|E|)$.

4 Experiments

In this section, we benchmark GRAPHGEN on real graph datasets and establish that:

- **Quality:** GRAPHGEN, on average, is significantly better than the state-of-the-art techniques of GraphRNN[40] and DeepGMG[19].
- **Scalability:** GRAPHGEN, on average, is 4 times faster than GraphRNN, which is currently the fastest generative model that works for labeled graphs. In addition, GRAPHGEN scales better with graph size, both in quality and efficiency.

The code and datasets used for our empirical evaluation can be downloaded from <https://github.com/idea-iitd/graphgen>.

4.1 Experimental setup

All experiments are performed on a machine running dual Intel Xeon Gold 6142 processor with 16 physical cores each, having 1 Nvidia 1080 Ti GPU card with 12GB GPU memory, and 384 GB RAM with Ubuntu 16.04 operating system.

4.1.1 Datasets Table 3 lists the various datasets used for our empirical evaluation. The semantics of the datasets are as follows.

- **Chemical compounds:** The first five datasets are chemical compounds. We convert them to labeled graphs where nodes represent atoms, edges represent bonds, node labels denote the atom-type, and edge labels encode the bond order such as single bond, double bond, etc.
- **Citation graphs:** Cora and Citeseer are citation networks; nodes correspond to publications and an edge represents one paper citing the other. Node labels represent the publication area.
- **Enzymes:** This dataset contains protein tertiary structures representing 600 enzymes from the BRENDA enzyme database[32]. Nodes in a graph (protein) represent secondary structure elements, and two nodes are connected if the corresponding elements are interacting. The node labels indicate the type of secondary structure, which is either helices, turns, or sheets. This is an interesting dataset since it contains only three label-types. We utilize this dataset to showcase the impact of graph invariants. Specifically, we supplement the node labels with node degrees. For example, if a node has label “A” and degree 5, we alter the label to “5, A”.

4.1.2 Baselines We compare GRAPHGEN with DeepGMG[19]¹ and GraphRNN[40]. For GraphRNN, we use the original code released

¹We modified the DeepGMG implementation for unlabeled graphs provided by Deep Graph Library (DGL)

by the authors. Since this code does not support labels, we extend the model to incorporate node and edge labels based on the discussion provided in the paper[40].

4.1.3 Parameters and Training sets For both GraphRNN and DeepGMG, we use the parameters recommended in the respective papers. Estimation of M in GraphRNN and evaluation of DFS codes² from graph database in GRAPHGEN is done in parallel using 48 threads.

For GRAPHGEN, we use 4 layers of LSTM cells for f_{trans} with hidden state dimension of 256 and the dimension of f_{emb} is set to 92. Hidden layers of size 512 are used in MLPs for f_{t_u} , f_{t_v} , f_{L_u} , f_e , f_{L_v} . We use *Adam optimizer* with a batch size of 32 for training. We use a dropout of $p = 0.2$ in MLP and LSTM layers. Furthermore, we use gradient clipping to remove exploding gradients and L2 regularizer to avoid over-fitting.

To evaluate the performance in any dataset, we split it into three parts: the train set, validation set, and test set. Unless specifically mentioned, the default split among training, validation and test is 80%, 10%, 10% of graphs respectively. We stop the training when validation loss is minimized or less than 0.05% change in validation loss is observed over an extended number of epochs. Note that both Citeseer and Cora represent a single graph. To form the training set in these datasets, we sample subgraphs by performing random walk with restarts from multiple nodes. More specifically, to sample a subgraph, we choose a node with probability proportional to its degree. Next, we initiate random walk with restarts with restart probability 0.15. The random walks stop after 150 iterations. Any edge that is sampled at least once during random walk with restarts is part of the sampled subgraph. This process is then repeated X times to form a dataset of X graphs. The sizes of the sampled subgraphs range from $1 \leq |V| \leq 102$ and $1 \leq |E| \leq 121$ in Citeseer and $9 \leq |V| \leq 111$ and $20 \leq |E| \leq 124$ in Cora.

4.1.4 Metrics The metrics used in the experiments can be classified into the following categories:

- **Structural metrics:** We use the metrics used by GraphRNN[40] for structural evaluation: (1) *node degree* distribution, (2) *clustering coefficient* distribution of nodes, and (3) *orbit count* distribution, which measures the number of all orbits with 4 nodes. Orbits capture higher-level motifs that are shared between generated and test graphs. The closer the distributions between the generated and test graphs, the better is the quality. In addition, we also compare the graph size of the generated graphs with the test graphs in terms of (4) *Average number of nodes* and (5) *Average number of edges*.
- **Label Accounting metrics:** We compare the distribution of (1) node labels, (2) edge labels, and (3) joint distribution of node labels and degree in generated and test graphs.
- **Graph Similarity:** To capture the similarity of generated graphs in a more holistic manner that considers both structure and labels, we use *Neighbourhood Sub-graph Pairwise Distance Kernel (NSPDK)*[6]. NSPDK measures the distance between two graphs by matching pairs of subgraphs with different radii and distances. The lower the NSPDK distance, the better is the performance. This quality metric is arguably the most important since it captures the global similarity instead of local individual properties.

²We adapted Minimum DFS code implementation from kaviniitm

Table 4: Summary of the performance by GRAPHGEN, GraphRNN, and DeepGMG across 11 different metrics measuring various aspects of quality, robustness and efficiency on 6 datasets. The best performance achieved under each metric for a particular dataset is highlighted in bold font. Any value less than 10^{-3} is reported as ≈ 0 . The quality achieved by DeepGMG in Enzymes, Cora, and Citeseer are not reported since loss function for DeepGMG goes to NAN and hence fails to scale.

Dataset	Model	Degree	Clustering	Orbit	NSPDK	Avg # Nodes (Gen/Gold)	Avg # Edges (Gen/Gold)	Node Label	Edge Label	Joint Node Label & Degree	Novelty	Uniqueness	Training Time	# Epochs
Lung	GRAPHGEN	0.009	≈ 0	≈ 0	0.035	35.20/35.88	36.66/37.65	0.001	≈ 0	0.205	$\approx 100\%$	$\approx 100\%$	6h	550
	GraphRNN	0.103	0.301	0.043	0.325	6.32/35.88	6.35/37.65	0.193	0.005	0.836	86%	45%	1d 1h	1900
	DeepGMG	0.123	0.001	0.026	0.260	11.04/35.88	10.28/37.65	0.083	0.002	0.842	98%	98%	23h	20
Yeast	GRAPHGEN	0.006	≈ 0	≈ 0	0.026	35.58/32.11	36.78/33.22	0.001	≈ 0	0.093	97%	99%	6h	250
	GraphRNN	0.512	0.153	0.026	0.597	26.58/32.11	27.01/33.22	0.310	0.002	0.997	93%	90%	21h	630
	DeepGMG	0.056	0.002	0.008	0.239	34.91/32.11	35.08/33.22	0.115	≈ 0	0.967	90%	89%	2d 3h	18
Mixed: Lung + Leukemia + Yeast + Breast	GRAPHGEN	0.005	≈ 0	≈ 0	0.023	37.87/37.6	39.24/39.14	0.001	≈ 0	0.140	97%	99%	11h	350
	GraphRNN	0.241	≈ 0	0.039	0.331	8.19/37.6	7.2/39.14	0.102	0.010	0.879	62%	52%	23h	400
	DeepGMG	0.074	0.002	0.002	0.221	24.35/37.6	24.11/39.14	0.092	0.002	0.912	83%	83%	1d 23h	11
Enzymes	GRAPHGEN	0.243	0.198	0.016	0.051	32.44/32.95	52.83/64.15	0.005	-	0.249	98%	99%	3h	4000
	GraphRNN	0.090	0.151	0.038	0.067	11.87/32.95	23.52/64.15	0.048	-	0.312	99%	97%	15h	20900
Citeseer	GRAPHGEN	0.089	0.083	0.100	0.020	35.99/48.56	41.81/59.14	0.024	-	0.032	83%	95%	4h	400
	GraphRNN	1.321	0.665	1.006	0.052	31.42/48.56	77.13/59.14	0.063	-	0.035	62%	100%	12h	1450
Cora	GRAPHGEN	0.061	0.117	0.089	0.012	48.66/58.39	55.82/68.61	0.017	-	0.013	91%	98%	4h	400
	GraphRNN	1.125	1.002	0.427	0.093	54.01/58.39	226.46/68.61	0.085	-	0.015	70%	93%	9h	400

• **Redundancy checks:** Consider a generative model that generates the exact same graphs that it saw in the training set. Although this model will perform very well in the above metrics, such a model is practically useless. Ideally, we would want the generated graphs to be diverse and similar, but not identical. To quantify this aspect, we check (1) *Novelty*, which measures the percentage of generated graphs that are not subgraphs of the training graphs and vice versa. Note that identical graphs are subgraph isomorphic to each other. In other words, novelty checks if the model has learned to generalize *unseen* graphs. We also compute (2) *Uniqueness*, which captures the diversity in generated graphs. To compute *Uniqueness*, we first remove the generated graphs that are subgraph isomorphic to some other generated graphs. The percentage of graphs remaining after this operation is defined as *Uniqueness*. For example, if the model generates 100 graphs, all of which are identical, the uniqueness is $1/100 = 1\%$.

To compute the distance between two distributions, like in GraphRNN[40], we use *Maximum Mean Discrepancy (MMD)*[11]. To quantify quality using a particular metric, we generate 2560 graphs and compare them with a random sample of 2560 test graphs. On all datasets except Enzymes, we report the average of 10 runs of computing metric, comparing 256 graphs in a single run. Since the Enzymes dataset contains only 575 graphs, we sample 64 graphs randomly from the test set 40 times and report the average.

4.2 Quality

Table 4 presents the quality achieved by all three benchmarked techniques across 10 different metrics on 6 datasets. We highlight the key observations that emerge from these experiments. Note that, some of the generated graphs may not adhere to the structural properties assumed in § 2 *i.e.*, no self loops, multiples edges or disconnected components, so we prune all the self edges and take the maximum connected component for each generated graph.

Graph and Sub-graph level similarity: On the NSPDK metric, which is the most important due to capturing the global similarity of generated graphs with test graphs, GRAPHGEN is significantly better across all datasets. This same trend also transfers to orbit count distributions. Orbit count captures the presence of motifs

also seen in the test set. These two metrics combined clearly establishes that GRAPHGEN model graphs better than GraphRNN and DeepGMG.

Node-level metrics: Among the other metrics, GRAPHGEN remains the dominant performer. To be more precise, GRAPHGEN is consistently the best in both Node and Edge Label preservation, as well as graph size in terms of the number of edges. It even performs the best on the joint Node Label and Degree metric, indicating its superiority in capturing structural and semantic information together. The performance of GRAPHGEN is comparatively less impressive in the Enzymes dataset, where GraphRNN marginally outperforms in the Degree and Clustering Coefficient metrics. Nonetheless, even in Enzyme, among the eight metrics, GRAPHGEN is better in six. This result also highlights the need to not rely on only node-level metrics. Specifically, although GraphRNN models the node degrees and clustering coefficients well, it generates graphs that are much smaller in size and hence the other metrics, including NSPDK, suffers.

Novelty and Uniqueness: Across all datasets, GRAPHGEN has uniqueness of at least 98%, which means it does not generate the same graph multiple times. In contrast, GraphRNN has a significantly lower uniqueness in chemical compound datasets. In Lung, only 45% of the generated graphs are unique. In several of the datasets, GraphRNN also has low novelty, indicating it regenerates graphs (or subgraphs) it saw during training. For example, in Cora, Citeseer and, the mixed chemical dataset, at least 30% of the generated graphs are regenerated from the training set. While we cannot pinpoint the reason behind this performance, training on random graph sequence representations could be a factor. More specifically, even though the generative model may generate new sequences, they may correspond to the same graph. While this is possible in GRAPHGEN as well, the likelihood is much less as it is trained on DFS codes that enable one-to-one mapping with graphs.

Analysis of GraphRNN and DeepGMG: Among GraphRNN and DeepGMG, DeepGMG generally performs better in most metrics. However, DeepGMG is extremely slow and fails to scale on larger networks due to $O(|V||E|^2)$ complexity.

GraphRNN’s major weakness is in learning graph sizes. As visible in Table 4, GraphRNN consistently generates graphs that are much smaller than the test graphs. We also observe that this issue

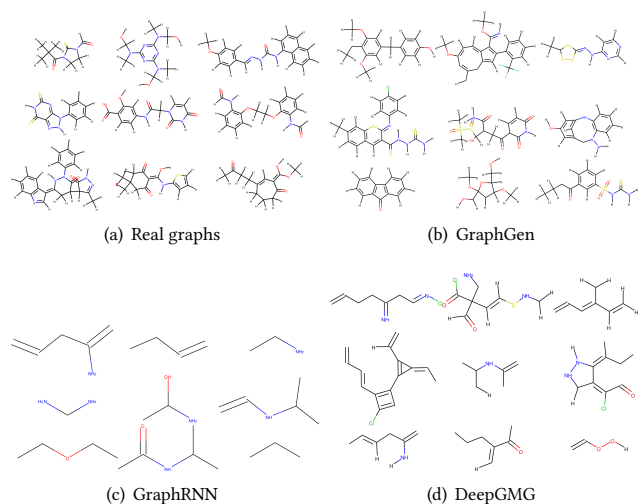


Figure 4: Visual comparison of the generated graphs with real graphs from the Lung dataset.

arises only in labeled graphs. If the labels are removed while retaining their structures, GraphRNN generates graphs that correctly mirror the test graph size distribution. This result clearly highlights that labels introduce an additional layer of complexity that simple extensions of models built for unlabeled graphs do not solve.

4.2.1 Visual Inspection To gain visual feedback on the quality of the generated graphs, in Fig. 4, we present a random sample of 9 graphs from the training set of Lung dataset and those generated by each of the techniques. Visually, GRAPHGEN looks the most similar, while GraphRNN is the most dissimilar. This result is consistent with the quantitative results obtained in Table 4. For example, consistent with our earlier observations, the GraphRNN graphs are much smaller in size and lack larger motifs like benzene rings. In contrast, GRAPHGEN’s graphs are of similar sizes and structures.

In Fig. 5, we perform the same exercise as above with 6 randomly picked graphs from the Cora dataset and those generated by GRAPHGEN and GraphRNN. Since the graphs in this dataset are much larger, it is hard to comment if GRAPHGEN is better than GraphRNN through visual inspection; the layout of a graph may bias our minds. However, we notice one aspect where GRAPHGEN performs well. Since Cora is a citation network, densely connected nodes (communities) have a high affinity towards working in the same publication area (node label/color). This correlation of label homogeneity with communities is also visible in GRAPHGEN(Fig. 5(b)).

4.3 Scalability

After establishing the clear superiority of GRAPHGEN in quality for labeled graph generative modeling, we turn our focus to scalability. To enable modeling of large graph databases, the training must complete within a reasonable time span. The penultimate column in Table 4 sheds light on the scalability of the three techniques. As clearly visible, GRAPHGEN is 2 to 5 times faster than GraphRNN, depending on the dataset. DeepGMG is clearly the slowest, which is consistent with its theoretical complexity of $O(|V||E|^2)$. If we

exclude the sequence generation aspect, GraphRNN has a lower time complexity for training than GRAPHGEN; while GraphRNN is linear to the number of nodes in the graph, GRAPHGEN is linear to the number of edges. However, GRAPHGEN is still able to achieve better performance due to training on canonical labels of graphs. In contrast, GraphRNN generates a random sequence representation for a graph in each epoch. Consequently, as shown in the last column of Table 4, GraphRNN runs for a far larger number of epochs to achieve loss minimization in the validation set. Note that DeepGMG converges within the minimum number of epochs. However, the time per epoch of DeepGMG is 100 to 200 times higher than GRAPHGEN. Compared to GraphRNN, the time per epoch of GRAPHGEN is $\approx 30\%$ faster on average.

4.3.1 Impact of Training Set Size To gain a deeper understanding of the scalability of GRAPHGEN, we next measure the impact of training set size on performance. Figs. 7(a)-7(b) present the growth of training times on ZINC and Cora against the number of graphs in the training set. While ZINC contains 3.2 million graphs, in Cora, we sample up to 1.2 million subgraphs from the original network for the training set. As visible, both GraphRNN and DeepGMG has a much steeper growth rate than GRAPHGEN. In fact, both these techniques fail to finish within 3 days for datasets exceeding 100,000 graphs. In contrast, GRAPHGEN finishes within two and a half days, even on a training set exceeding 3 million graphs. The training times of all techniques are higher in Cora since the graphs in this dataset are much larger in size. We also observe that the growth rate of GRAPHGEN slows at larger training sizes. On investigating further, we observe that with higher training set sizes, the number of epochs required to reach the validation loss minima reduces. Consequently, we observe the trend visible in Figs. 7(a)-7(b). This result is not surprising since the learning per epoch is higher with larger training sets.

An obvious question arises at this juncture: *Does lack of scalability to larger training sets hurt the quality of GraphRNN and DeepGMG?* Figs. 7(c)-7(e) answer this question. In both ZINC and Cora, we see a steep improvement in the quality (reduction in NSPDK and Orbit) of GraphRNN as the training size is increased from $\approx 10,000$ graphs to $\approx 50,000$ graphs. The improvement rate of GRAPHGEN is relatively milder, which indicates that GraphRNN has a greater need for larger training sets. However, this requirement is not met as GraphRNN fails to finish within 3 days, even for 100,000 graphs. Overall, this result establishes that scalability is not only important for higher productivity but also improved modeling.

4.3.2 Impact of Graph Size We next evaluate how the size of the graph itself affects the quality and training time. Towards that end, we partition graphs in a dataset into multiple buckets based on its size. Next, we train and test on each of these buckets individually and measure the impact on quality and efficiency. Figs. 7(f) and 7(h) present the impact on quality in chemical compounds (same as Mixed dataset in Table 4) and Cora respectively. In both datasets, each bucket contains exactly 10,000 graphs. The size of graphs in each bucket is however different, as shown in the x -axis of Figs. 7(f) and 7(h). Note that Cora contains larger graphs since the network itself is much larger than chemical compounds. The result for DeepGMG is missing on the larger graph-size buckets since it

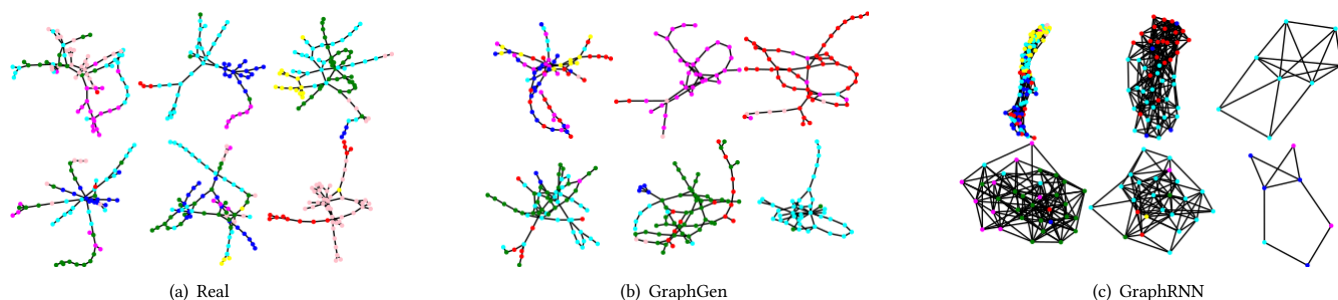


Figure 5: Visual comparison of the generated graphs with real graphs from Cora. In this figure, the colors of the nodes denote their labels.

fails to model large graphs. GraphRNN runs out of GPU memory (12GB) in the largest bucket size in Cora.

As visible, there is a clear drop in quality (increase in NSPDK) as the graph sizes grow. This result is expected since larger graphs involve larger output spaces, and the larger the output space, the more complex is the modeling task. Furthermore, both GRAPHGEN and GraphRNN convert graph modeling into sequence modeling. It is well known from the literature that auto-regressive neural models struggle to learn *long-term* dependencies in sequences. When the sequence lengths are large, this limitation impacts the quality. Nonetheless, GRAPHGEN has a more gradual decrease in quality compared to GraphRNN and DeepGMG.

Next, we analyze the impact of graph size on the training time. Theoretically, we expect the training time to grow, and this pattern is reflected in Figs. 7(g) and 7(i). Note that the y -axis is in log scale in these plots. Consistent with previous results, GRAPHGEN is faster. In addition to the overall running time, we also show the average time taken by GRAPHGEN in computing the minimum DFS code. Recall that the worst-case complexity of this task is factorial to the number of nodes in the graph. However, we earlier argued that in practice, the running times are much smaller. This experiment adds credence to this claim by showing that DFS code generation is a small portion of the total running time. For example, in the largest size bucket of chemical compounds, DFS code generation of all 10,000 graphs take 30 seconds out of the total training time of 4 hours. In Cora, on the largest bucket size of 500 edges, the DFS construction component consumes 50 minutes out of the total

training time of 10 hours. GraphRNN has a similar pre-processing component as well (GraphRNN-M), where it generates a large number of BFS sequences to estimate a hyper-parameter. We find that this pre-processing time, although of polynomial-time complexity, is slower than minimum DFS code computation in chemical compounds. Overall, the results of this experiment support the proposed strategy of feeding canonical labels to the neural model instead of random sequence representations.

4.4 Impact of Invariants

Minimum DFS code generation relies on the node and edge labels to prune the search space and identify the lexicographically smallest code quickly. When graphs are unlabeled or have very few labels, this process may become more expensive. In such situations, labels based on vertex invariants allow us to augment existing labels. To showcase this aspect, we use the Enzymes dataset, which has only 3 node labels and no edge labels. We study the training time and the impact on quality based on the vertex invariants used to label nodes. We study four combinations: (1) existing node labels only, (2) node label + node degree, (3) node label + clustering coefficient (CC), and (4) label + degree + CC. Fig. 6 presents the results. As visible, there is a steady decrease in the DFS code generation time as more invariants are used. No such trend, however, is visible in the total training time as additional features may both increase or decrease the time taken by the optimizer to find the validation loss minima. From the quality perspective, both NSPDK and Orbit show improvement (reduction) through the use of invariants. Between degree and CC, degree provides slightly improved results. Overall, this experiment shows that invariants are useful in both improving the quality and reducing the cost of minimum DFS code generation.

4.5 Alternatives to LSTMs

For deep, auto-regressive modeling of sequences, we design an LSTM tailored for DFS codes. *Can other neural architectures be used instead? Since a large volume of work has been done in the NLP community on sentence modeling, can those algorithms be used by treating each edge tuple as a word?* To answer these questions, we replace LSTM with SentenceVAE[5] and measure the performance. We present the results only in Lung and Cora due to space constraints; a similar trend is observed in other datasets as well. In Table 5, we present the two metrics that best summarize the impact of this experiment. As clearly visible, SentenceVAE introduces a

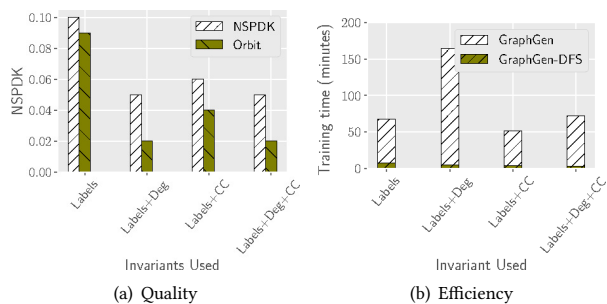


Figure 6: Impact of vertex invariants on (a) quality and (b) training time on Enzymes dataset

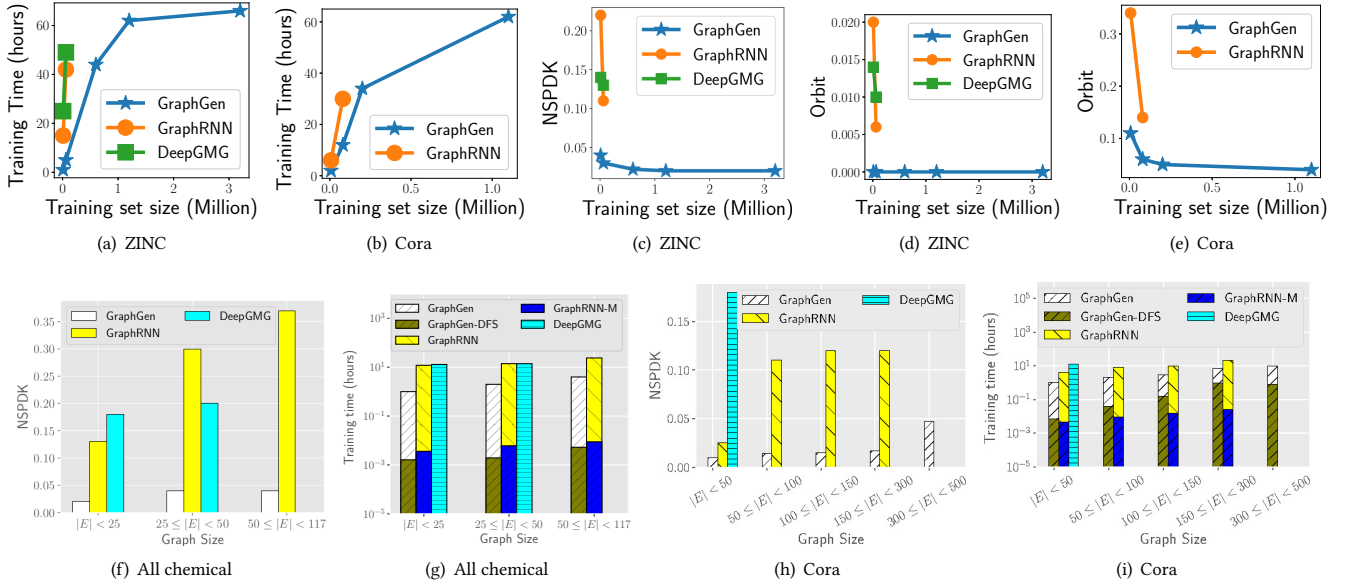


Figure 7: Impact of training set size on (a-b) efficiency and (c-e) quality. Impact of graph size on (f, h) quality and (g, i) training time. The y -axis of (g) and (i) are in log scale.

huge increase in NSPDK distance, which means inferior quality. An even more significant result is observed in Uniqueness, which is close to 0 for SentenceVAE. This means the same structure is repeatedly generated by SentenceVAE. In DFS codes, every tuple is unique due to the timestamps, and hence sentence modeling techniques that rely on repetition of words and phrases, fail to perform well. While this result does not say that LSTMs are the only choice, it does indicate the need for architectures that are custom-made for DFS codes.

5 Concluding Insights

In this paper, we studied the problem of learning generative models for labeled graphs in a domain-agnostic and scalable manner. There are two key takeaways from the conducted study. First, existing techniques model graphs either through their adjacency matrices or sequence representations. In both cases, the mapping from a graph to its representation is one-to-many. Existing models feed multiple representations of the same graph to the model and rely on the model overcoming this information redundancy. In contrast, we construct canonical labels of graphs in the form of minimum DFS codes and reduce the learning complexity. Canonical label construction has non-polynomial time complexity, which could be a factor behind this approach not being adequately explored. Our study shows that although the worst-case complexity is factorial to the number of nodes, by exploiting nodes/edge labels, and vertex invariants, DFS-code construction is a small component of the overall training time (Figs. 7(g) and 7(i)). Consequently, the time

complexity of graph canonization is not a practical concern and, feeding more precise graph representations to the training model is a better approach in terms of quality and scalability.

The second takeaway is the importance of quality metrics. Evaluating graph quality is a complicated task due to the multi-faceted nature of labeled structures. It is, therefore, important to deploy enough metrics that cover all aspects of graphs such as local node-level properties, structural properties in the form of motifs and global similarity, graph sizes, node and edge labels, and redundancy in the generated graphs. A learned model is effective only if it performs well across all of the metrics. As shown in this study, GRAPHGEN satisfies this criteria.

The conducted study does not solve all problems related to graph modeling. Several graphs today are annotated with feature vectors. Examples include property graphs and knowledge graphs. Can we extend label modeling to feature vectors? All of the existing learning-based techniques, including GRAPHGEN, cannot scale to graphs containing millions of nodes. Can we overcome this limitation? We plan to explore these questions further by extending the platform provided by GRAPHGEN.

Acknowledgments

The authors thank Lovish Madaan for helpful discussions and comments on the paper. The authors also thank IIT Delhi HPC facility for the computational resources.

Table 5: LSTM Vs. SentenceVAE.

Technique	Lung		Cora	
	NSPDK	Uniqueness	NSPDK	Uniqueness
LSTM	0.03	≈ 100%	0.012	98%
SentenceVAE	0.7	0.4%	0.78	0.4%

References

- [1] Edoardo M. Airoldi, David M. Blei, Stephen E. Fienberg, and Eric P. Xing. 2008. Mixed Membership Stochastic Blockmodels. *J. Mach. Learn. Res.* 9 (2008), 1981–2014.
- [2] R.Álka Albert and Albert-László Barabási. 2002. Statistical mechanics of complex networks. *Reviews of Modern Physics* 74, 1 (Jan. 2002), 47–97.
- [3] Prithu Banerjee, Pranali Yawalkar, and Sayan Ranu. 2016. Mantra: a scalable approach to mining temporally anomalous sub-trajectories. In *ACM SIGKDD*. 1415–1424.
- [4] Karsten M. Borgwardt, Cheng Soon Ong, Stefan Schönauer, S. V. N. Vishwanathan, Alexander J. Smola, and Hans-Peter Kriegel. 2005. Protein function prediction via graph kernels. *Bioinformatics* 21 Suppl 1 (2005), i47–56.
- [5] Samuel R. Bowman, Luke Vilnis, Oriol Vinyals, Andrew M. Dai, Rafal Józefowicz, and Samy Bengio. 2016. Generating Sentences from a Continuous Space. In *Proceedings of the 20th SIGNLL Conference on Computational Natural Language Learning, CoNLL 2016, Berlin, Germany, August 11-12, 2016*, Yoav Goldberg and Stefan Riezler (Eds.), 10–21.
- [6] Fabrizio Costa and Kurt De Grave. 2010. Fast Neighborhood Subgraph Pairwise Distance Kernel. In *ICML*. 255–262. <https://icml.cc/Conferences/2010/papers/347.pdf>
- [7] Nicola De Cao and Thomas Kipf. 2018. MolGAN: An implicit generative model for small molecular graphs. *ICML 2018 workshop on Theoretical Foundations and Applications of Deep Generative Models* (2018).
- [8] Shuangfei Fan and Bert Huang. 2019. Labeled Graph Generative Adversarial Networks. *CoRR* abs/1906.03220 (2019).
- [9] Alex Graves, Santiago Fernández, Marcus Liwicki, Horst Bunke, and Jürgen Schmidhuber. 2007. Unconstrained On-line Handwriting Recognition with Recurrent Neural Networks. In *NIPS*. 577–584.
- [10] Alex Graves, Abdel-rahman Mohamed, and Geoffrey E. Hinton. 2013. Speech recognition with deep recurrent neural networks. In *ICASSP*. IEEE, 6645–6649.
- [11] Arthur Gretton, Karsten M. Borgwardt, Malte J. Rasch, Bernhard Schölkopf, and Alexander J. Smola. 2012. A Kernel Two-Sample Test. *J. Mach. Learn. Res.* 13 (2012), 723–773.
- [12] Aditya Grover, Aaron Zweig, and Stefano Ermon. 2019. Graphite: Iterative Generative Modeling of Graphs. In *ICML*. 2434–2444.
- [13] Sepp Hochreiter and Jürgen Schmidhuber. 1997. Long Short-Term Memory. *Neural Computation* 9, 8 (1997), 1735–1780.
- [14] John J. Irwin and Brian K. Shoichet. 2005. ZINC A Free Database of Commercially Available Compounds for Virtual Screening. *Journal of Chemical Information and Modeling* 45, 1 (2005), 177–182.
- [15] Wengong Jin, Regina Barzilay, and Tommi S. Jaakkola. 2018. Junction Tree Variational Autoencoder for Molecular Graph Generation. In *ICML (Proceedings of Machine Learning Research)*, Jennifer G. Dy and Andreas Krause (Eds.), Vol. 80. 2328–2337.
- [16] Wataru Kawai, Yusuke Mukuta, and Tatsuya Harada. 2019. GRAM: Scalable Generative Models for Graphs with Graph Attention Mechanism. *CoRR* abs/1906.01861 (2019).
- [17] Michihiro Kuramochi and George Karypis. 2004. An Efficient Algorithm for Discovering Frequent Subgraphs. *IEEE Trans. Knowl. Data Eng.* 16, 9 (2004), 1038–1051.
- [18] Jure Leskovec, Deepayan Chakrabarti, Jon M. Kleinberg, Christos Faloutsos, and Zoubin Ghahramani. 2010. Kronecker Graphs: An Approach to Modeling Networks. *J. Mach. Learn. Res.* 11 (2010), 985–1042.
- [19] Yujia Li, Oriol Vinyals, Chris Dyer, Razvan Pascanu, and Peter W. Battaglia. 2018. Learning Deep Generative Models of Graphs. *CoRR* abs/1803.03324 (2018).
- [20] Yibo Li, Liangren Zhang, and Zhenming Liu. 2018. Multi-objective de novo drug design with conditional graph generative model. *J. Cheminformatics* 10, 1 (2018), 33:1–33:24.
- [21] Renjie Liao, Yujia Li, Yang Song, Shenlong Wang, William L. Hamilton, David Duvenaud, Raquel Urtasun, and Richard S. Zemel. 2019. Efficient Graph Generation with Graph Recurrent Attention Networks. In *NeurIPS*. 4257–4267.
- [22] Qi Liu, Miltiadis Allamanis, Marc Brockschmidt, and Alexander L. Gaunt. 2018. Constrained Graph Variational Autoencoders for Molecule Design. In *NeurIPS*, Samy Bengio, Hanna M. Wallach, Hugo Larochelle, Kristen Grauman, Nicolò Cesa-Bianchi, and Roman Garnett (Eds.), 7806–7815.
- [23] U.S. National Library of Medicine National Center for Biotechnology Information. [n.d.]. *PubChem*. <http://pubchem.ncbi.nlm.nih.gov>
- [24] Mariya Popova, Mykhailo Shvets, Junier Oliva, and Olexandr Isayev. 2019. MolecularRNN: Generating realistic molecular graphs with optimized properties. *CoRR* abs/1905.13372 (2019).
- [25] Sayan Ranu, Bradley T. Calhoun, Ambuj K. Singh, and S. Joshua Swamidass. 2011. Probabilistic Substructure Mining From Small-Molecule Screens. *Molecular Informatics* 30, 9 (2011), 809–815.
- [26] Sayan Ranu and Ambuj K. Singh. 2009. GraphSig: A Scalable Approach to Mining Significant Subgraphs in Large Graph Databases. In *ICDE*. 844–855.
- [27] Sayan Ranu and Ambuj K Singh. 2009. Mining Statistically Significant Molecular Substructures for Efficient Molecular Classification. *Journal of Chemical Information and Modeling* 49 (2009), 2537–2550.
- [28] Alfréd Rényi. 1959. On random graphs. *Publ. Math. Debrecen*. v6 (1959), 290–297.
- [29] Garry Robins, Tom A. B. Snijders, Peng Wang, Mark Handcock, and Philippa Pattison. 2007. Recent developments in exponential random graph (p*) models for social networks. *Social Networks* 29 (2007), 192–215.
- [30] Hojjat Salehinejad, Sharan Sankar, Joseph Barfett, Errol Colak, and Shahrokh Valaee. 2017. Recent Advances in Recurrent Neural Networks. *arXiv e-prints* (Dec 2017).
- [31] Bidisha Samanta, Abir De, Gourhari Jana, Pratim Kumar Chattaraj, Niloy Ganguly, and Manuel Gomez Rodriguez. 2019. NeVAE: A Deep Generative Model for Molecular Graphs. In *AAAI*. 1110–1117.
- [32] Ida Schomburg, Antje Chang, Christian Ebeling, Marion Gremse, Christian Heldt, Gregor Huhn, and Dietmar Schomburg. 2004. BRENDA, the enzyme database: updates and major new developments. *Nucleic acids research* 32 Database issue (2004), D431–3.
- [33] Prithviraj Sen, Galileo Namata, Mustafa Bilgic, Lise Getoor, Brian Gallagher, and Tina Eliassi-Rad. 2008. Collective Classification in Network Data. *AI Magazine* 29, 3 (2008), 93–106.
- [34] Martin Simonovsky and Nikos Komodakis. 2018. GraphVAE: Towards Generation of Small Graphs Using Variational Autoencoders. In *Artificial Neural Networks and Machine Learning - ICANN 2018 - 27th International Conference on Artificial Neural Networks, Rhodes, Greece, October 4-7, 2018, Proceedings, Part I (Lecture Notes in Computer Science)*, Vera Kurková, Yannis Manolopoulos, Barbara Hammer, Lazaros S. Iliadis, and Ilias Maglogiannis (Eds.), Vol. 11139. 412–422.
- [35] Cong Tran, Won-Yong Shin, Andreas Spitz, and Michael Gertz. 2019. DeepNC: Deep Generative Network Completion. *CoRR* abs/1907.07381 (2019).
- [36] Hongwei Wang, Jia Wang, Jialin Wang, Miao Zhao, Weinan Zhang, Fuzheng Zhang, Xing Xie, and Minyi Guo. 2018. GraphGAN: Graph Representation Learning With Generative Adversarial Nets. In *AAAI-18*. 2508–2515.
- [37] Duncan J. Watts and Steven H. Strogatz. 1998. Collective dynamics of 'small-world' networks. *Nature* 393, 6684 (June 1998), 440–442.
- [38] Xifeng Yan and Jiawei Han. 2002. gSpan: Graph-Based Substructure Pattern Mining. In *Proceedings of the 2002 IEEE International Conference on Data Mining (ICDM 2002), 9-12 December 2002, Maebashi City, Japan*. 721–724.
- [39] Jiaxuan You, Bowen Liu, Zhitao Ying, Vijay S. Pande, and Jure Leskovec. 2018. Graph Convolutional Policy Network for Goal-Directed Molecular Graph Generation. In *Advances in Neural Information Processing Systems 31: Annual Conference on Neural Information Processing Systems 2018, NeurIPS 2018, 3-8 December 2018, Montréal, Canada*. 6412–6422.
- [40] Jiaxuan You, Rex Ying, Xiang Ren, William L. Hamilton, and Jure Leskovec. 2018. GraphRNN: Generating Realistic Graphs with Deep Auto-regressive Models. In *Proceedings of the 35th International Conference on Machine Learning, ICML 2018, Stockholm, Sweden, July 10-15, 2018 (Proceedings of Machine Learning Research)*, Jennifer G. Dy and Andreas Krause (Eds.), Vol. 80. PMLR, 5694–5703.
- [41] Muhan Zhang, Shali Jiang, Zhicheng Cui, Roman Garnett, and Yixin Chen. 2019. D-VAE: A Variational Autoencoder for Directed Acyclic Graphs. *CoRR* abs/1904.11088 (2019).